ROCKET MEASUREMENTS OF AURORAL-ZONE ENERGETIC ELECTRONS AT SYOWA STATION, ANTARCTICA

II. CHARACTERISTICS OF ELECTRONS UNDER ACTIVE AURORAL CONDITIONS

Masahiro KODAMA,

Yamanashi Medical College, Tamaho-mura, Nakakoma-gun, Yamanashi 409-38

Shoko KUDO, Masami WADA, Hajime TAKEUCHI, Takashi IMAI

The Institute of Physical and Chemical Research, 7-13, Kaga 1-chome, Itabashi-ku, Tokyo 173

and

Hisao YAMAGISHI

National Institute of Polar Research Institute, 9-10, Kaga 1-chome, Itabashi-ku, Tokyo 173

Abstract: Some fundamental properties of auroral electrons with energies greater than 40 keV were measured by a series of seven sounding rockets launched from Syowa Station, Antarctica, during the IMS period of 1976–78. The payload consists of a set of proportional counter and plastic scintillation counter covering several fixed energy bands. Measurements under different conditions of active aurora were carried out four times in the altitude range of 70 to 220 km. The observation results are discussed in comparison with those given by the other three quiet-time measurements, in terms of altitude profile, pitch angle distribution and energy spectrum. Principal characters of behavior of energetic electrons based on the comparative studies are summarized as follows: a) A peak in the intensity-altitude profile appears around 120 km in altitude at disturbed time, counting rates being 5×10^5/cm^2·s·sr·keV for 40 keV electrons in maximum, while the profile at quiet time is saturated at a counting rate of 10^3/cm^2·s·sr·keV. b) Pitch angle distribution changes from the field-trapped mode in quiet condition into the field-aligned one at disturbed time. c) The value of power law exponent of energy spectrum is found to be 7–8 at disturbed time, while about 4 at quiet time.

1. Introduction

One of the important subjects of studies of auroral phenomena is to solve mechanism of production and acceleration of precipitating auroral particles, particularly of high-energy electrons of the order of 10^3 to 10^5 eV, which appear abruptly in contrast with the normally existing radiation belt particles of less than 10^3 eV. In

order to explore this problem, extensive measurements of electrons by means of rockets and polar-orbiting satellites have been performed so far. Most of them aimed to measure mainly low energy electrons from 10^3 to 10^4 eV which occupy the majority of the so-called auroral particles. In fact, some new evidences of auroral electrons have been found from these measurements, for example, field-aligned electrons (HOFFMAN and EVANS, 1968; WHALEN and MCDIARMID, 1973), monoenergetic peak in spectrum (EVANS, 1967), inverted-V structure in energy-time spectrogram (ACKERSON and FRANK, 1972), and Birkeland's current-particle relation (CASSERLY and CLOUTIER, 1975; CARLSON and KELLEY, 1977).

However, a search for behavior of highly energetic electrons with over a few 10^4 eV will give an important information directly connected to acceleration or precipitation process of auroral particles. Also, it will play an essential role in the comparative studies over a waide energy range with other interesting auroral phenomena such as ionospheric electron density profile, cosmic noise absorption and auroral luminosity.

At Syowa Station, Antarctica (69°00'S, 39°35'E), the first rocket experiment to measure energetic auroral electrons started in January 1976 and then six similar flights followed by August 1978. Four and three flights of them were made under disturbed and quiet conditions, respectively. Details of the results obtained by the first flight experiment were already given as part I (KODAMA *et al.*, 1978), and some preliminary reports on the others followed (OKUTANI *et al.*, 1979; WADA *et al.*, 1979; KODAMA *et al.*, 1980).

The purpose of this paper is to summarise transient modulations of a few characteristic features of energetic electrons between quiet and disturbed conditions, by comparing the respective three flights with each other, excepting one of the disturbed-time flights, S-310JA-6, which recorded abnormally low electron fluxes. The results of this work are compared with some results of nine similar rocket experiments in the northern hemisphere, covering the equivalent energy and altitude regions to the Syowa flights. Detailed discussions by taking into account the three-dimensional relationship between the rocket trajectory and bright auroral arcs will be given elsewhere.

2. Description of the Flights and the Geophysical Conditions

General specifications of the sounding rockets at Syowa Station, from which the electron data discussed here were obtained, are listed in Table 1, including some geophysical parameters implying the degree of auroral activity. Two types of the single-staged rockets, S-210 and S-310 were used. Four rockets of serial Nos. 2, 3, 5 and 7 were launched under disturbed conditions as shown in Table 1, and Nos. 1, 4 and 6 rockets at quiet time.

Fig. 1 shows the trajectories of the rockets, where they are projected on the geomagnetic meridian plane passing through Syowa Station. One can easily estimate

Table 1. List of sounding rockets at Syowa Station.

No.	Rocket	Launching time (LT)	Maximum altitude (km)	Scanning pitch angle	Electron flux*	*Kp*-index	ΔH** (γ)	CNA*** (dB)
1.	S-210JA-22	0220 Jan. 26, 1976	119	6°–141°	1×10^3	1−	0	0
2.	-20	0240 June 25, 1976	118	40°–140°	4×10^4	4+	150	0.3
3.	-21	0323 July 26, 1976	116	50°–130°	4×10^4	3−	20	0.2
4.	-23	0731 Sep. 13, 1976	120	22°–157°	5×10^3	1+	0	0
5.	S-310JA-2	0322 Feb. 10, 1977	212	12°–118°	5×10^5	3+	500	0.7
6.	-3	1835 July 26, 1977	222	56°–74°	3×10^3	1+	0	0
7.	-6	0056 Aug. 28, 1978	237	28°–62°, 73°–107°	1×10^3	4	200	0.1

* Counts/cm²·s·sr·keV at 40 keV. ** Geomagnetic horizontal component. *** 30 MHz cosmic noise absorption.

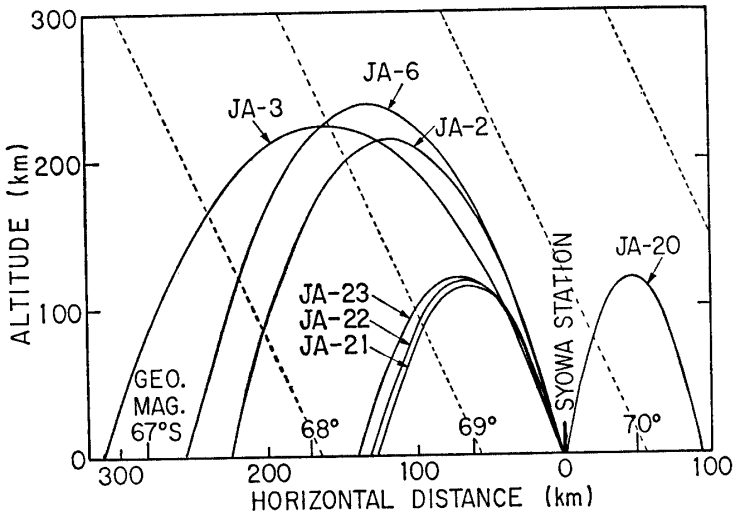

Fig. 1. Rocket trajectories projected on the geomagnetic meridian plane passing through Syowa Station.

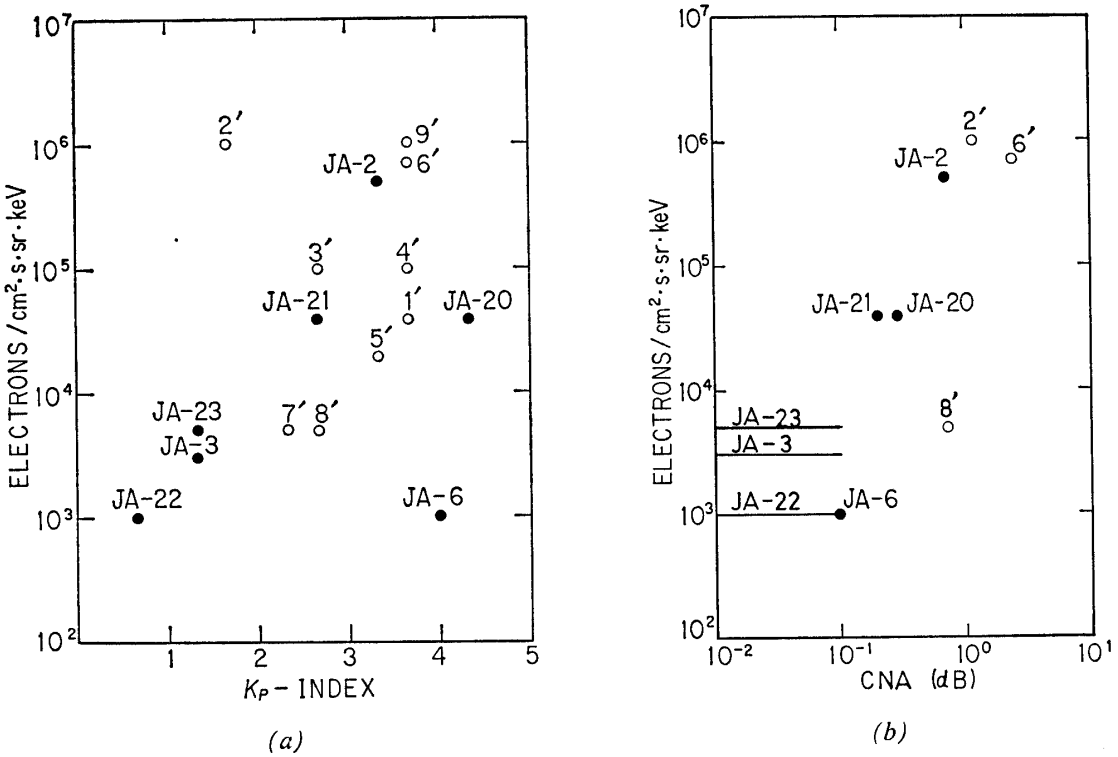

Fig. 2. Correlation diagrams of electron fluxes at 40 keV against a) Kp-index and b) 30 MHz cosmic noise absorption. Solid and open circles are for the rockets at Syowa Station and the northern hemisphere rockets, respectively.

Table 2. List of sounding rockets in the northern hemisphere.

No.	Authors	Launching time (LT)	Launching site	Maximum altitude (km)	Electron flux*	*Kp*-index	ΔH** (γ)	CNA*** (dB)
1′.	LAMPTON (1967)	0944 Sep. 17, 1965	Ft. Churchill	140	4×10^4	4−		
2′.	EVANS (1967)	2256 Feb. 17, 1966	〃	188	1×10^6	2−	200	1.2
3′.	OGILVIE (1968)	2355 Apr. 13, 1966	〃	250	(1×10^5)	3−		
4′.	WESTERLUND (1969)	2347 Mar. 17, 1967	〃	790	(1×10^5)	4−		
5′.	REARWIN (1971)	2253 Apr. 23, 1968	〃	200	(2×10^4)	3+	335	2.5
6′.	CARLSON and KELLEY (1977)	2259 Apr. 2, 1970	〃	557	7×10^5	4−	400	
7′.	CLOUTIER *et al.* (1973)	2217 Feb. 13, 1971	Pokar Flat	210	(5×10^3)	2+	80	
8′.	WHALEN and MCDIARMID (1973)	2132 Feb. 19, 1971	Ft. Churchill		(5×10^3)	3−	200	0.7
9′.	PAZICH and ANDERSON (1975)	2122 Feb. 24, 1972	Pokar Flat	200	1×10^6	4−		

* Counts/cm²·s·sr·keV at 40 keV, ( ): extrapolated. ** Geomagnetic horizontal component. *** 30 MHz cosmic noise absorption.

from the figure the successive changes of the mutual relation between the flying location of a rocket and the magnetic lines of force.

Maximum fluxes of 40 keV electrons observed are shown in Table 1, together with some indices of geomagnetic disturbance. Figs. 2a and 2b show the correlation diagrams of the electron fluxes against *Kp*-index and 30 MHz cosmic noise absorption (CNA), respectively, where some electron data available from the northern hemisphere rocket experiments (Table 2) are plotted together. It seems reasonable that the wide scattering of points as seen in Fig. 2a becomes less in Fig. 2b, because the energetic electron precipitation should be better correlated with the CNA observed near the rocket launching site. In particular, we note a better contribution of two peculiar points, 2′ and JA-6, of Fig. 2a to Fig. 2b. Though the CNA data collection is not good enough, this roughly suggests that the electron measurements in this series of rocket experiment at Syowa Station were performed successfully.

3. Payload Instrumentation

The rocket-borne electron detectors are disc-shaped type plastic scintillation counters and thin mica window type proportional counters. Details of their geometrical factors were described in Part I (KODAMA *et al.*, 1978). Quite the same specification of the both detectors was used for each of all rockets except S-310JA-6 (No. 7), but the number of the detectors and their on-board arrangement are somewhat different from rocket to rocket, as shown in Table 3. The rockets JA-22, -23 and -6 had two sets of proportional counters, mounted with the different angles (45° and 90°) against the rocket axis. The rockets JA-2 and -3 had a duplicate set of the both types of counters, *i.e.*, with and without magnetic shielding collimator, in order to search possible contributions of bremsstrahlung photons to the respective detectors. The rocket JA-6 used a thinner mica window for the proportional counter, so that the detectable threshold energy was reduced to 25 keV.

From the combination of the detector arrangement and the spinning and coning motions of the rocket, the measurable pitch angles of precipitating electrons are determined definitely. The actual full scanning range of pitch angle is listed in Table 1.

Since the heights of pulse signals from the counter vary depending on the energy of incoming electrons, individual pulse heights were discriminated into three or four energy bands as shown in Table 3, and hence the total number of data channels given in the table was achieved.

The data of each channel were sampled every 50 ms and then converted into the analogue signals corresponding to four digit code. The converted data were transmitted by the FM/FM telemeter system during the following 50 ms interval. The sampling rates for the highest energy bands, PC-BG and SC-BG, except 65° M* of Table 3, were one second respectively, because of a limitation of the telemeter response. The detailed description of the above on-board data processing was given

by WADA *et al.* (1979), including the data reduction through an analogue-to-digital conversion in the laboratory.

Table 3. Mounted angles and energy channels of rocket-borne electron detectors.

No.	Proportional counter (PC)						Scintillation counter (SC)			Number of data channels
	PC-L 40–60 keV	PC-L 25–30 keV	PC-H 60–110 keV	PC-ML 30–50 keV	PC-MH 50–100 keV	PC-BG 110 keV	SC-L 60-80 keV	SC-H 80–170 keV	SC-BG 170 keV	
S-210JA-22, 23	45°, 90°						90°			7
S-210JA-20, 21	90°						90°			5
S-310JA-2, 3	65°						65°			12
	65°M*						65°M*			
		PC-L 25–30 keV		PC-ML 30–50 keV	PC-MH 50–100 keV	PC-H 100–200 keV				
S-310JA-6		45°, 90°								8

* With 1200 gauss permanent magnet to reject electrons with energies less than 200 keV.

4. Results and Discussions

4.1. *Intensity-altitude profile*

The altitude profile of electron flux depends not only on energy but also on auroral activity which varies temporally and/or spatially, particularly on the three-dimensional relative situation between the location of a rocket and active auroral arcs. If the rocket flies across the different lines of the constant L-values as in the descent course of most of flights, it also may modulate the observed profile. The observed electron fluxes were accumulated over a unit time interval longer than the spin period so as to eliminate their possible change due to the spin modulation.

Figs. 3a and 3b show the selected two examples of 1-s electron counts in the energy ranges of 40–60 keV and 80–170 keV respectively. In the lower energy band, it is seen from Fig. 3a that the overall fluxes observed by the disturbed-time flights, JA-20, -21 and -2, are higher than those by the quiet-time flights. In addition, the flux at the maximum altitude becomes higher in the order of the rockets JA-21, -20 and -2. It is of interest that this order of enhancement is consistent with that of the electron density observed simultaneously using the Langmuir probe by OGAWA *et al.* (1978).

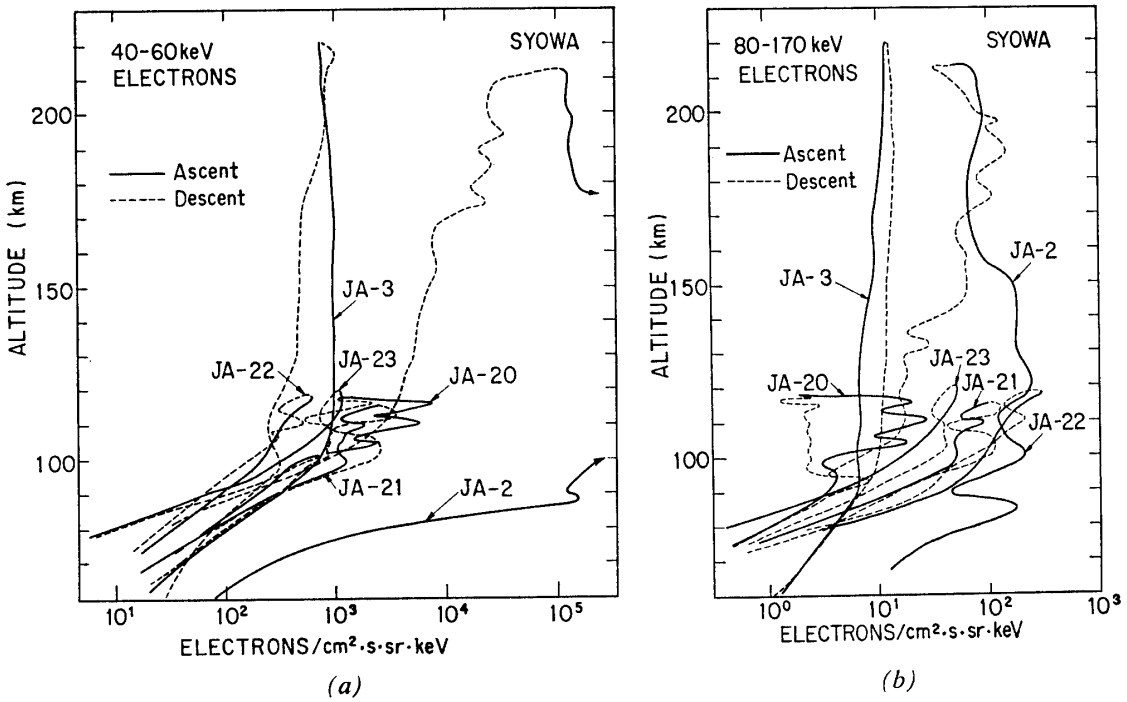

Fig. 3. Altitude profiles of electron fluxes in the energy ranges of a) 40–60 keV and b) 80–170 keV, during the entire flight of each of six rockets at Syowa Station.

As for the three flights of the S-310 rockets, there is a considerable difference in fluxes between the ascent and descent flights. One of the reasons for this difference may be attributed to the lowering of the L-value by 1.3 to 1.6 with the time elapse after launch, as seen from the rocket trajectories in Fig. 1. Another one is probably due to the rocket's flying away from the active auroral arcs with time, in the light of all-sky camera photographs. The ascent-descent difference is no longer clear in the higher energy region of Fig. 3b. This may indicate that the electrons with energies as high as the order of 100 keV are not always directly related to auroral activity.

The rocket JA-2 was launched during the most intense auroral activity throughout this series of experiment. Let us examine the details of its altitude profiles sorted by pitch angles. Since the counting rates in the lowest energy channel PC-L were unfortunately over-saturated in the altitude range of 100–170 km during the ascent flight, the altitude profile from the moderate energy range 60–80 keV is shown in Fig. 4, where Figs. 4a and 4b are for the ascent and descent flights, respectively. It is clearly seen from Fig. 4a that a peak flux in the profile appears around 120 km in altitude regardless of pitch angles. This altitude coincides with the so-called auroral altitude generally defined by optical observations. As described later, both the flattening of pitch angle distribution and the softening of energy spectrum are predominant there. Hence, it is plausible to consider that the peak profile was caused by a considerable amount of increment of lower energy electrons contributable to auroral luminosity. Such a profile is in contrast with the flat profile observed by the quiet-time rocket JA-3. During the descent flight, no more peak appeared at the

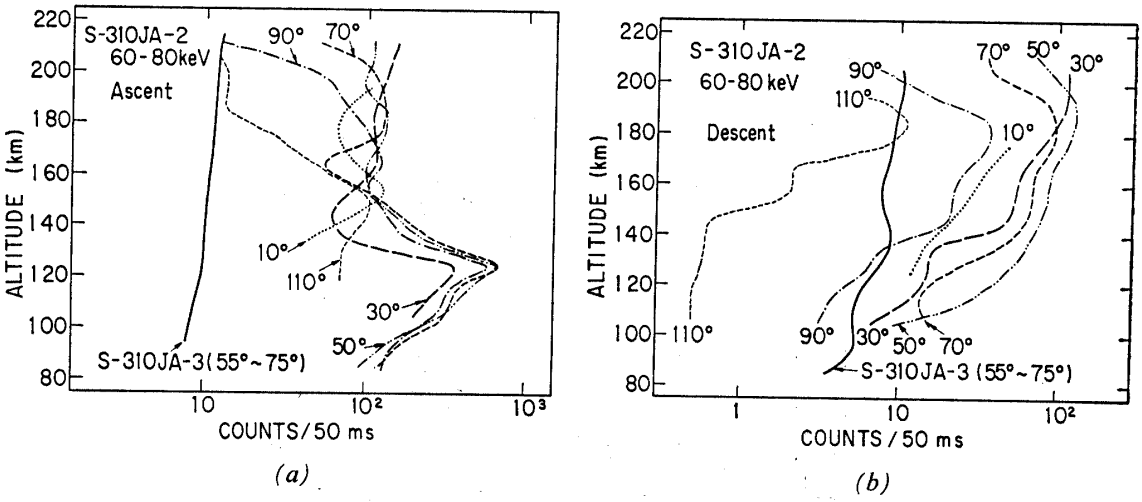

Fig. 4. Pitch angle sorted altitude profiles of electron fluxes in the energy range 60–80 keV, where a) ascent and b) descent flights. A solid curve is for the rocket JA-3, inclusive pitch angles from 55° to 75°, and the others for the JA-2. Note the different offset of the ordinate scale between a) and b).

same altitude and overall fluxes successively approached to the background flux by the rocket JA-3, because of successive lowering of the L-value and dislocation of the rocket far from the active auroral arc region.

Next, how about the pitch angle dependence of the altitude profile under disturbed condition? The pitch angle sorted altitude profile of Fig. 4 implies that such dependence is appreciable with increasing altitudes, and fluxes of the 50°–70° pitch angle component are predominant during the descent flight. In the altitude range below 120 km, two disturbed-time rockets JA-20 and -21 also gave significant pitch angle dependences as shown in Figs. 5 and 6, which suggest steeper altitude profiles

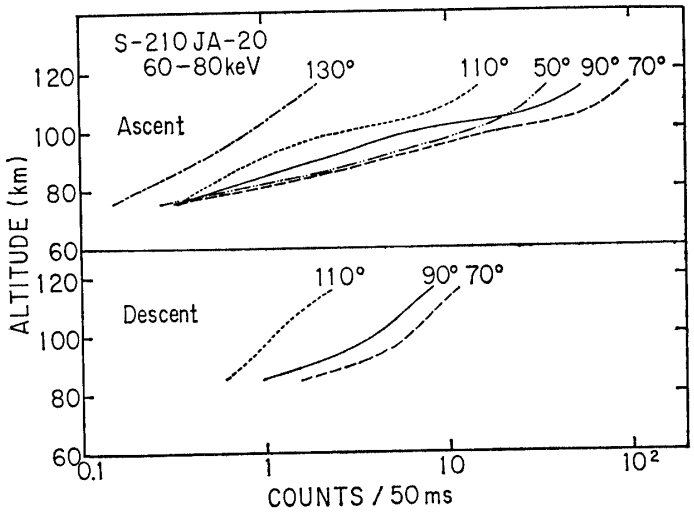

Fig. 5. Pitch angle sorted altitude profiles of electron fluxes in the energy range 60–80 keV observed by the rocket JA-20.

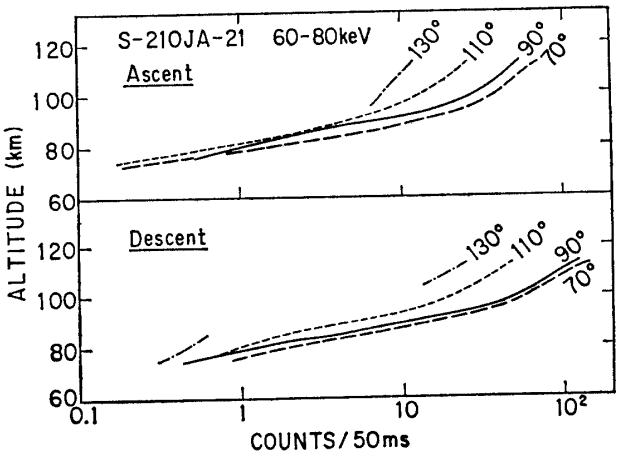

Fig. 6. Pitch angle sorted altitude profiles of electron fluxes in the energy range 60–80 keV observed by the rocket JA-21.

for the 70°–90° pitch angle components. Therefore, it should be noted that a fractional contribution of the electrons with smaller pitch angles increases with the increment of altitude. This will be more clearly proved in the light of the pitch angle distribution which follows below.

4.2. Pitch angle distribution

The combination of rocket spinning and precession motions during the flight allows a definite scanning range of pitch angles to be viewed by the detectors. As the spinning and precession data are available from the on-board magnetic aspect sensor, it is possible to deduce the averaged flux of electrons over a selected small range of pitch angle or at any pitch angle, by calculating the angle between the pointing direction of detector and the magnetic line of force. The minimum range of the pitch angle was taken as 5° actually, taking into account the half aperture angle of the detectors, 20°, and the data sampling time of 50 ms.

During an active auroral disturbance, a typical example of the pitch angle distributions of energetic electrons covering ranges of energy and altitude as wide as possible was obtained by the rocket JA-2. Fig. 7 shows a number of pitch angle distributions deduced from the data accumulated every 10 km ranges of altitude, for each of the different three energy channels. Results from the descent flight alone

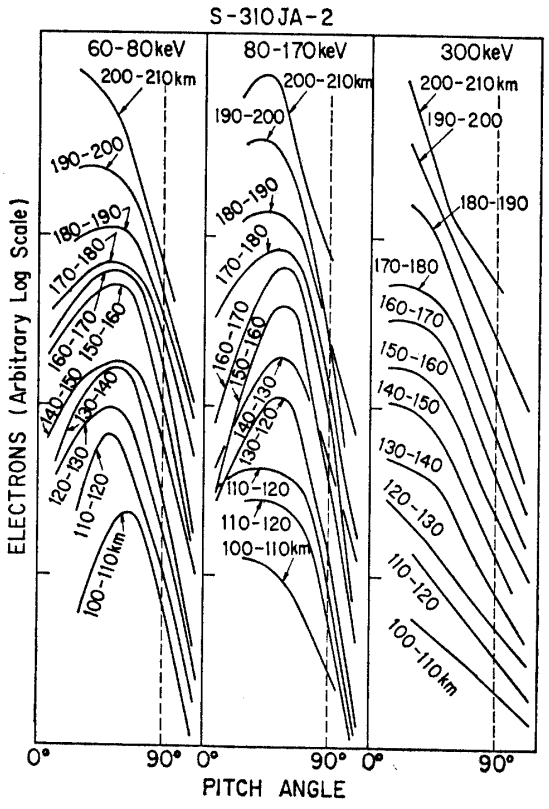

Fig. 7. Altitude dependences of pitch angle distributions of electrons observed during the descent flight of the rocket JA-2. The curves are shifted arbitrarily for clear illustrations. The distributions in the different three energy channels are given.

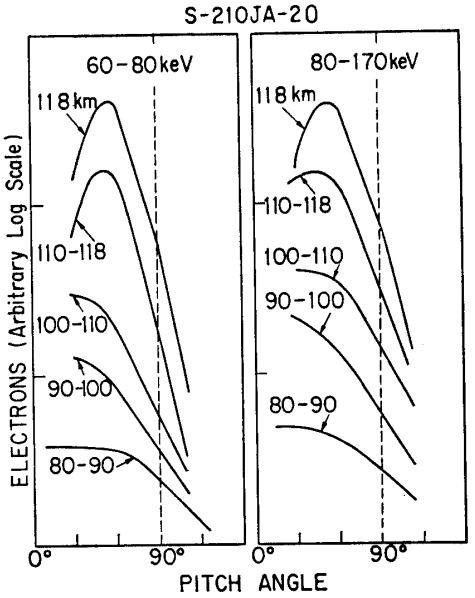

Fig. 8. Altitude dependences of pitch angle distributions of electrons during the ascent flight of the rocket JA-20.

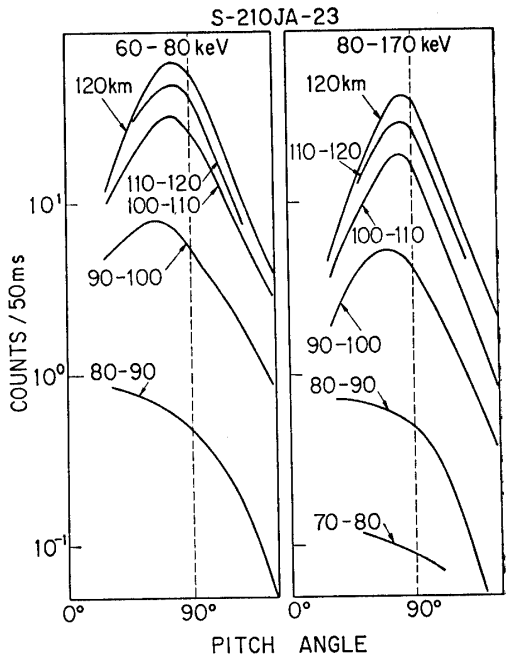

Fig. 9. Altitude dependences of pitch angle distributions of electrons during the ascent flight of the rocket JA-23.

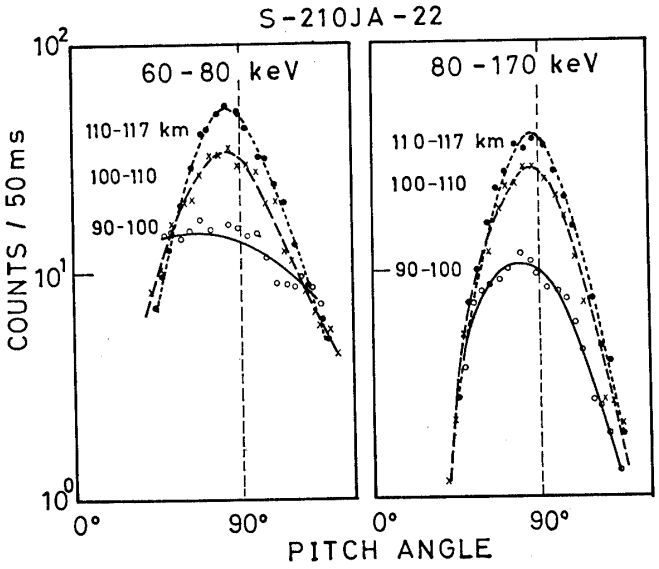

Fig. 10. Altitude dependences of pitch angle distributions of electrons during the ascent flight of the rocket JA-22.

were adopted here, because the counting rate saturation happened to occur in the proportional counter during the ascent flight. It is evident from the figure that the peaked pitch angle, in which the maximum electron flux was recorded, decreases gradually from near 60° to the smaller angles with increasing altitude. This tendency is more remarkable for the lower energy ranges, and there are no significant peak and no systematic altitude dependence in the energy range greater than 300 keV. The other two disturbed-time rockets, JA-20 and -21, also showed the altitude variation of pitch angle distribution which is consistent with the above, although the measuring altitude was limited to a narrow range of 70–120 km. Fig. 8 shows the results of the rocket JA-20, in which the peaked pitch angle is found around 60° in the altitude range of 100–120 km. Though the peak position seems to shift to the smaller in lower altitudes less than 100 km, it is not always significant due to the poorer counting statistics.

It is of interest to compare the above characteristics with those by the quiet-time measurements. Fig. 9, one of such measurements, shows the altitude and energy dependences of the pitch angle distributions observed by the rocket JA-23. A different point of these from Fig. 8 is that the position of a peak in the distribution is found near 90° at any altitude and energy. Another quiet-time example by the rocket JA-22 also showed the similar character that the field-trapped type of electrons are usually dominant, as seen in Fig. 10. Unfortunately, the quiet-time rocket JA-3, which attained to the highest altitude of 222 km, gave no satisfactory pitch angle distribution covering the wider pitch angle range, due to the stable flight with small precession motion. There is, therefore, no evidence to support that the characteristics seen in Fig. 9 are valid even in the higher altitudes above 120 km. If this is true, it can be concluded that the most probable pitch angle of energetic electrons precipitating into the auroral region is found near 90° at quiet time, while at disturbed time it changes from about 60° in the so-called auroral altitude of 110–120 km to the smaller angles in the higher altitudes.

According to the northern hemisphere rocket experiments of energetic electrons with energies less than 20 keV, it is believed that there exist occasionally the field-aligned electrons highly collimated having pitch angles less than 20° (ARNOLDY *et al.*, 1974). To account for this high degree of field alignment with the monoenergetic character, a possibility of local acceleration by electric fields was invoked. In some cases, 6–8 keV electron flux rose from pitch angle of 0° to 60° and then dropped sharply toward greater pitch angles (PAZICH and ANDERSON, 1975).

Fig. 11 shows a summary of the pitch angle distributions obtained by the rockets at Syowa Station, including LAMPTON's (1967) result which is an example of those by the northern hemisphere observations of electrons with a comparable order of energy to the present work. In the northern hemisphere (Ft. Churchill), the electron flux at disturbed time remains sharply peaked near 90° in the energy range of 60–150 keV, except a very late phase in the flight when atmospheric scattering is appreciable.

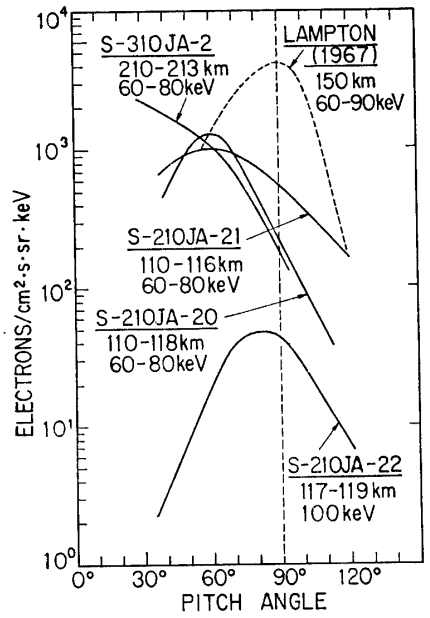

Fig. 11. Pitch angle distributions of energetic electrons observed in the northern hemisphere and at Syowa Station. The rocket JA-22 was launched at quiet time while the others under disturbed conditions.

Also, the enhanced precipitation is fractionally greater at smaller pitch angles. On the other hand, at Syowa Station, the similar pattern to the above is recognized in the case of the quiet-time result (JA-22 in Fig. 10), but the disturbed-time results reveal a distinct lower shift of the peaked pitch angle. Considering the precipitation relation for a particle with a constant velocity along a magnetic line of force,

$$\frac{\sin^2\alpha}{B}=\text{const.}, \tag{1}$$

where α is a pitch angle in the geomagnetic field B, this fact seems to be associated with the anomalously low geomagnetic field intensity in the vicinity of Syowa Station, which leads us to unusual lowering of the mirroring altitude of particles.

4.3. Energy spectrum

Since the number of the different energy channels available in the present experiments is limited and their energy interval is comparatively wide, it is convenient to deduce the energy spectrum by assuming its functional form. When a spectral function is expressed by $f(E)$, a count ratio R between selected any two channels is given by

$$R=\frac{\int_{E_1}^{E_2} f(E)\mathrm{d}E}{\int_{E_3}^{E_4} f(E)\mathrm{d}E}, \tag{2}$$

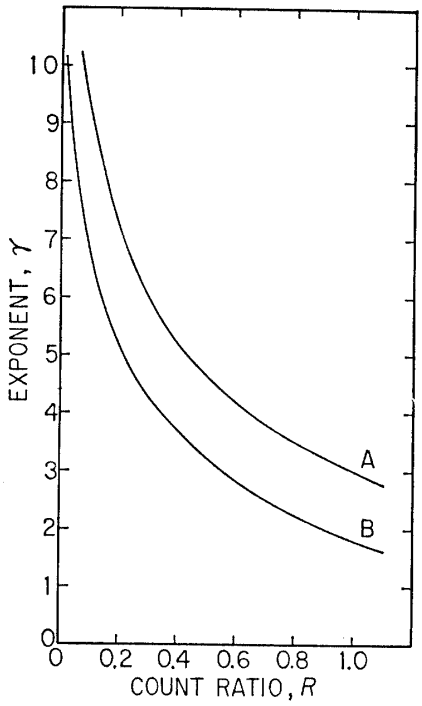

Fig. 12. The power law exponent of the energy spectrum as a function of R, which is a count ratio between any two different energy channels. Curve A is obtained from the combination of the energy channels SC-H and SC-L, and curve B for the pair of PC-H and PC-L channels.

where E_1 and E_2 are the lower and upper limiting energies of one channel, respectively, and E_3 and E_4 are those for the other. From eq. (2) we obtain the values of R by assuming a function of $f(E)$ for the combination of any two energy channels. When the power law spectrum of $f(E)=aE^{-\gamma}$ is assumed, R is given by

$$R=\frac{E_1^{-(\gamma-1)}-E_2^{-(\gamma-1)}}{E_3^{-(\gamma-1)}-E_4^{-(\gamma-1)}}. \tag{3}$$

Fig. 12 shows two examples of the R values calculated by using eq. (3) as a function of γ.

The power law spectral exponents as functions of pitch angle and altitude thus calculated are shown in Figs. 13 and 14 as disturbed-time examples. The exponents were obtained from the combination of the SC-H and SC-L channels. An interesting point found in Fig. 14a is considerable softening of the energy spectrum, around the auroral altitude of 110–120 km, in which the maximum enhanced flux was recorded as seen in Fig. 14a. This softening also has a remarkable pitch angle dependence, being appreciable at greater pitch angle. In higher altitudes greater than 140 km, the values of the exponent largely fluctuate similar to the measurement by JOHNSTONE and DAVIS (1974). The rocket JA-20 in Fig. 14a demonstrates a distinct and systematic altitude profile of the exponent at the altitudes less than 120 km. The exponent there increases by at least 4 with increasing altitudes. After all, the exponent amounts to 8 to 9 in maximum at disturbed time.

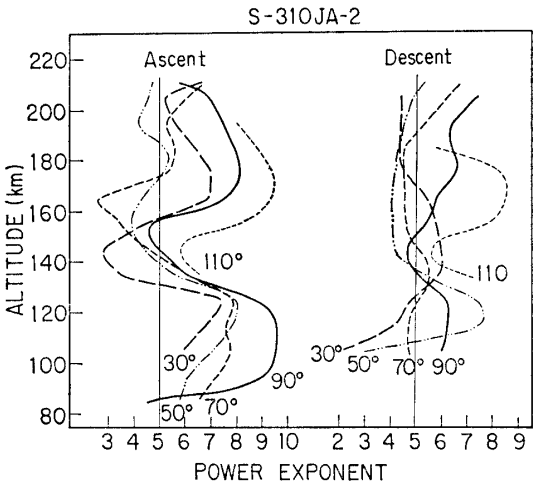

Fig. 13. Pitch angle sorted altitude dependences of the exponent of the power law energy spectrum measured in the rocket JA-2. The exponents plotted here are those calculated by a pair of the SC-H and SC-L energy channels.

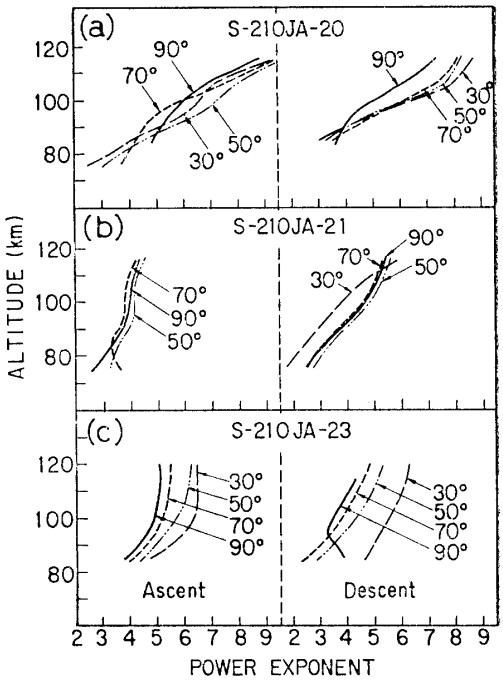

Fig. 14. Pitch angle sorted altitude dependences of the exponent of the power law energy spectrum. The exponents plotted here are those calculated by a pair of the SC-H and SC-L energy channels. (a) the rocket JA-20, (b) the rocket JA-21 and (c) the rocket JA-23.

On the contrary, the exponent remains in the range of 4 to 5 at quiet-time, as seen in Fig. 14c. The pitch angle dependence also is noted, that is, the greater is the pitch angle, the smaller the exponent at any altitude. The same analysis of the rocket JA-22 gave the similar character of pitch angle dependence, where the exponent varies from 4.0 to 5.7 against the pitch angle change from 90° to 10° (KODAMA *et al.*, 1978). Since the JA-21 sample in Fig. 14b is rather similar to the quiet-time profile of Fig. 14c, it suggests that the energy spectrum during this auroral event was harder than that in the other disturbed events.

It is worth-while to compare the above-mentioned energy spectrum of energetic electrons with that of low energy electrons less than 10 keV. The latter was observed simultaneously by KUBO *et al.* (1979) in the rocket JA-2 experiment. Both the spectra obtained at 213 km in altitude are shown in Fig. 15, where the absolute fluxes of electrons having pitch angles of 10° and 20°–60° for lower and higher energy ranges, respectively, are plotted. It is estimated from a comparison in absolute fluxes that

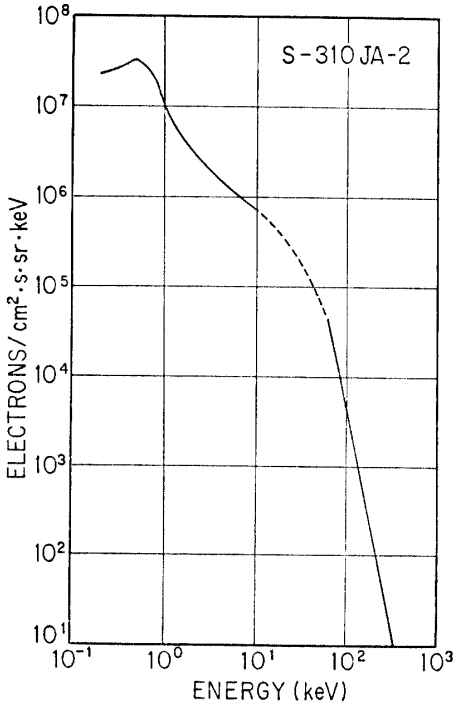

Fig. 15. Energy spectra of low- and high-energy electrons measured simultaneously by the rocket JA-2 at 213 km in altitude. Pitch angles of electrons are 10° for the former and 20°–60° for the latter, respectively.

the two spectra are connected consistently with each other despite of a partial lack of the spectrum between them.

In the calculations of the spectral exponent, there occurred occasionally a discrepancy between any two pairs of the different energy channels, particularly between the different two detectors of plastic and proportional counters. This may be attributed to a possible difference in the detection efficiency between the two counters, including the relative sensitivity to photons. In fact, an apparent influence of photon contribution to the proportional counter was observed partly during the flight JA-20, on the basis of spin modulation analysis, and also observed by a comparison between the magnetic-shield and the non-shield detectors during the flight JA-2 (KODAMA *et al.*, 1980). Accordingly, the exponents described above were calculated from the same pair of energy channels, SC-H and SC-L, throughout all the flights.

5. Summary of Observations

The data obtained from this experiment can be summarized in terms of three fundamental physical properties of energetic electrons.

Intensity-altitude profile

1. At quiet time, the flux remains nearly constant in higher altitudes greater than 120 km, giving the background flux of 10^3/cm²·s·sr·keV in the 40–60 keV range and of 10^3/cm²·s·sr·keV in the 80–170 keV range.

2. At disturbed time, the maximum flux is found around 120 km in altitude, showing the enhancements of $10^5/cm^2 \cdot s \cdot sr \cdot keV$ or greater and $10^2/cm^2 \cdot s \cdot sr \cdot keV$ in the 40–60 keV and 80–170 keV ranges, respectively.

3. The electrons having pitch angle near 90° have most dominant dependence against altitude.

Pitch angle distribution

1. At quiet time, the pitch angle distribution shows a peaked flux at pitch angle near 90°, regardless of energy and altitude.

2. At disturbed time, the peak position in the pitch angle distribution exists near 60° at an altitude of 120 km or less and it shifts toward the lower pitch angles with increasing altitude and/or with enhancement of auroral disturbance.

Energy spectrum

1. At quiet time, the exponent of the power law spectrum is found to be 4 to 5 and is kept almost constant against altitude.

2. The exponent becomes somewhat larger at smaller pitch angles, by a factor of 1 for the pitch angle range from 90° to 30°.

3. At disturbed time, the exponent is enhanced up to 7 to 8 near 120 km in altitude, and it becomes 4 to 6 above and below there, with some pitch angle dependence.

6. Conclusion

In this work, a point of analysis was mainly placed not on spatial but on temporal characters. It was assumed that the observed variations of electron fluxes were due to time variations of auroral activity at the first approximation. In order to examine strictly the spatial characters, it is of importance to deal with the data by taking into account the spatial relation between the rocket trajectory and auroral arcs, because some of the flights, JA-2 and -21, revealed the evidence of crossing active auroral bands (HIRASAWA, 1980, private communication). Moreover, a particular notice should be paid to the systematic change of the L-value along the trajectory. Further investigations introducing these parameters will be reported in the near future.

The authors wish to express our hearty thanks to the rocket experiment members of the 17th, 18th and 19th Japanese Antarctic Research Expeditions for their efforts in launching the rockets at Syowa Station. We also thank Drs. T. HIRASAWA and H. FUKUNISHI of the National Institute of Polar Research for providing the geophysical and auroral data. The IMS campaign for the rocket experiments was organized by the National Institute of Polar Research.

References

ACKERSON, K. L. and FRANK, L. A. (1972): Correlated satellite measurements of low-energy electron

precipitation and ground-based observations of a visible auroral arc. J. Geophys. Res., **77**, 1128–1136.

ARNOLDY, R. L., LEWIS, P. B. and ISAACSON, P. O. (1974): Field-aligned auroral electron fluxes. J. Geophys. Res., **79**, 4208–4221.

CARLSON, C. W. and KELLEY, M. C. (1977): Observation and interpretation of particle and electric field measurements inside and adjacent to an active auroral arc. J. Geophys. Res., **82**, 2349–2360.

CASSERLY, R. T. and CLOUTIER, P. A. (1975): Rocket-based magnetic observations of auroral Birkeland currents in association with a structured auroral arc. J. Geophys. Res., **80**, 2165–2168.

CLOUTIER, P. A., SANDEL, B. R., ANDERSON, H. R., PAZICH, P. M. and SPIGER, R. J. (1973): Measurement of auroral Birkeland currents and energetic particle fluxes. J. Geophys. Res., **78**, 640–647.

EVANS, D. S. (1967): A 10-cps periodicity in the precipitation of auroral-zone electrons. J. Geophys. Res., **72**, 4281–4291.

HOFFMAN, R. A. and EVANS, D. S. (1968): Field-aligned electron bursts at high altitudes observed by OGO 4. J. Geophys. Res., **73**, 6201–6214.

JOHNSTONE, A. D. and DAVIS, T. N. (1974): Low-altitude acceleration of auroral electrons during breakup observed by a mother-daugher rocket. J. Geophys. Res., **79**, 1416–1425.

KODAMA, M., IMAI, T., TAKEUCHI, H. and WADA, M. (1978). Rocket measurements of auroral-zone energetic electrons at Syowa Station, Antarctica. I. Characteristics of electrons under no geomagnetic disturbance. Mem. Natl Inst. Polar Res., Spec. Issue, **9**, 11–23.

KODAMA, M., OKUTANI, S., WADA, M., IMAI, T. and TAKEUCHI, H. (1980): Roketto kôdo ni okeru >40 keV ôrora denshi no picchi-kaku bunpu (Pitch angle distribution of >40 keV auroral electrons observed at rocket altitudes). Nankyoku Shiryô (Antarct. Rec.), **68**, 35–46.

KUBO, H., MURATA, S., ITOH, T. and KOKUBUN, S. (1979): S-310JA-2-gôki ni yoru kôka denshi no kansoku (Observation of precipitating electrons on board the S-310JA-2). Nankyoku Shiryô (Antarct. Rec.), **63**, 17–28.

LAMPTON, M. (1967): Daytime observations of energetic auroral zone electrons. J. Geophys. Res., **72**, 5817–5823.

OGAWA, T., MORI, H. and MIYAZAKI, S. (1978): Electron density and temperature profiles in the Antarctic auroral ionosphere observed by sounding rockets. J. Radio Res. Labs., **25**, 73–94.

OGILVIE, K. W. (1968): Auroral electron energy spectra. J. Geophys. Res., **73**, 2325–2332.

OKUTANI, S., WADA, M., TAKEUCHI, H., KODAMA, M. and IMAI, T. (1979): Nankyoku roketto ni yoru ôrora-tai kôka denshi no kansoku (Observations of auroral-zone precipitating electrons by the Antarctic rockets). Nankyoku Shiryô (Antarct. Rec.), **63**, 29–41.

PAZICH, P. M. and ANDERSON, H. R. (1975): Rocket measurement of auroral electron fluxes associated with field-aligned currents. J. Geophys. Res., **80**, 2152–2160.

REARWIN, S. (1971): Rocket measurements of low-energy auroral electrons. J. Geophys. Res., **76**, 4505–4517.

WADA, M., OKUTANI, S., IMAI, T., TAKEUCHI, H. and KODAMA, M. (1979): Ôrora denshi kansoku shiryô shori (Data processing for auroral electron analysis). Nankyoku Shiryô (Antarct. Rec.), **63**, 53–59.

WESTERLUND, L. H. (1969): The auroral electron energy spectrum extended to 45 eV. J. Geophys. Res., **74**, 351–354.

WHALEN, B. A. and MCDIARMID, I. B. (1973): Pitch angle diffusion of low-energy auroral electrons. J. Geophys. Res., **78**, 1608–1614.

(Received September 1, 1980; Revised manuscript received January 8, 1981)